Hygrothermal characterization of lightweight biosourced composites based on date palm fiber and lime

Abdelhafid Gherfi, A. Merabet, R. Belakroum, M. Kadja, T. Moussa, M. Lachi, G. Polidori, C. Maalouf

Hygrothermal characterization of lightweight biosourced composites based on date palm fiber and lime

A. Gherfi[1,2], A. Merabet[3], R. Belakroum[2], M. Kadja[4], T. Moussa[5], M. Lachi[5], G. Polidori[5], C. Maalouf[5]

[1]Mechanical Engineering Department, Faculty of Science and Technology, University Constantine 1, Constantine 25000, Algeria

[2]Univ. Ouargla, Fac. des Sciences Appliquées, Lab. Dynamique, Interaction et Réactivité des Systèmes, Ouargla 30000, Algeria

[3]Mechanical laboratory, Mechanical Engineering Department, Faculty of Science and Technology, University Constantine 1,   Constantine 25000, Algeria

[4]Laboratoire d'énergétique appliquée et pollution, Université de Constantine I, Constantine 25000, Algeria

[5] Groupe de Recherche en Sciences pour l'Ingénieur /Thermomécanique (EA 4694), Université de Reims Champagne-Ardenne, France

ABSTRACT

Biosourced materials derived from agricultural by-products hold significant promise in both enhancing the hygrothermal performance of buildings and reducing their environmental footprint. We investigate the hygrothermal properties of green composites based on date palm fibers and lime. The eco-friendly building composites explored are manufactured using either trunk fiber (surface fiber) or rachi and petiole fiber (wood fiber). Through an experimental approach, for different fiber percentages, the hygrothermal characteristics of the explored composites were experimentally determined in terms of thermal conductivity, diffusivity, porosity, water vapor permeability, and sorption scanning isotherms. The results show that date palm fiber has a positive effect on the thermal properties of the composite material. Indeed, it significantly enhances the insulating capacity of the composites. Water vapor permeability exhibits significant variation depending on the fiber content, with samples containing higher fiber content exhibiting greater permeability. Furthermore, the Effective Moisture Penetration Depth (EMPD) model proved effective describing the experimental adsorption scanning isotherm curves. It was observed that the sorption process is significantly

influenced by both the type and percentage of fibers. Finally, the observed results demonstrate that date palm fiber and lime composites could offer notable advantages for construction applications and serve as an effective, cost-effective insulation.

Keywords: Date palm fiber, Lime, Hygrothermal properties, Moisture permeability, Relative humidity

1. Introduction

For ecologic and economic reasons, converting agriculture wastes to environmentally-friendly construction materials have gained a lot of interest recently. Date Palm Fibers (DPF) are a natural and renewable product with excellent thermophysical and acoustic properties for the development of efficient insulating materials (Braiek et al., 2017). Algeria is one of the largest producers of date palms in the world, totaling a palm grove area of more than 160,000 ha with 18.6 million date palms, and date production generates about 200,000 tons of waste per year (Bellatrache et al., 2020).

For the past two decades, research on the potential uses of date palm fibers has surged, attracting significant attention. It has shown that date palm fibers are suitable reinforcements in many composite materials, such as polymeric, phenolic, and epoxy composites. This adaptability has been demonstrated in various studies (Al-Oqla & Sapuan, 2014; Asim et al., 2021; Asim et al., 2020; Asyraf et al., 2022; Kannan & Thangaraju, 2021; Mahdi et al., 2019; Supian et al., 2021). Research has revealed **the** promising potential of date palm fibers in construction materials, particularly cement-based mortars. Numerous studies have explored the benefits of integrating this sustainable resource, highlighting its positive impact on material properties (Benaimeche et al., 2018; Benmansour et al., 2014; Boukhattem et al., 2017; Chennouf et al., 2018; Haba et al., 2017; Vantadori et al., 2019; Zanichelli et al., 2018). Furthermore, recent studies have explored the potential of incorporating date palm fiber into

Compressed Earth Blocks (CEBs) to improve their mechanical and hygrothermal properties (Atiki et al., 2021; Subramanian et al., 2021; Taallah & Guettala, 2016; Taallah et al., 2014).

To the best of our knowledge, only two studies have explored the properties of a lime based matrix reinforced by date palm fiber. Belakroum et al. (2017) explored bio-composites based on date palm fiber and lime or starch. Through the results reported in their study, the explored samples have shown good acoustic absorption performances and demonstrated the capacity of such composites to regulate indoor relative humidity variations. Belakroum et al. (2018) presented an experimental investigation of eco-materials based on surface date palm fiber (mesh fiber) and lime. The experiments on the elaborated material investigated its mechanical, thermal, acoustic properties and moisture buffering capacity. The analysis revealed the significant potential for the utilization of the DPF-lime composite as an insulation material due to its multifunctional capacities.

The present study investigates two date palm fiber-lime composites. These materials differ in their type of date palm fiber: one is made of crushed surface fiber (mesh fibers) and the other one is made of crushed wood fiber (rachis fiber). We have conducted experiments on three different formulations of each type of material. By means of experimental methods, we have explored the thermal conductivity, the thermal diffusivity, the open porosity, the density, the water vapor permeability, and the moisture sorption scanning isotherms.

2. Material and methods

From a date palm, we can produce four types of fiber (Alotaibi et al., 2019). These fibers come from the trunk, rachis, petiole, and palm fruit branches, as illustrated in Figure 1. In this study, for producing the biocomposites, we used two types of date palm fibers: the first one from crushing the mesh layer, which surrounds the trunk known as Surface Fiber (SF) and the second one results from crushing dried petioles also called Wood Fiber (WF).
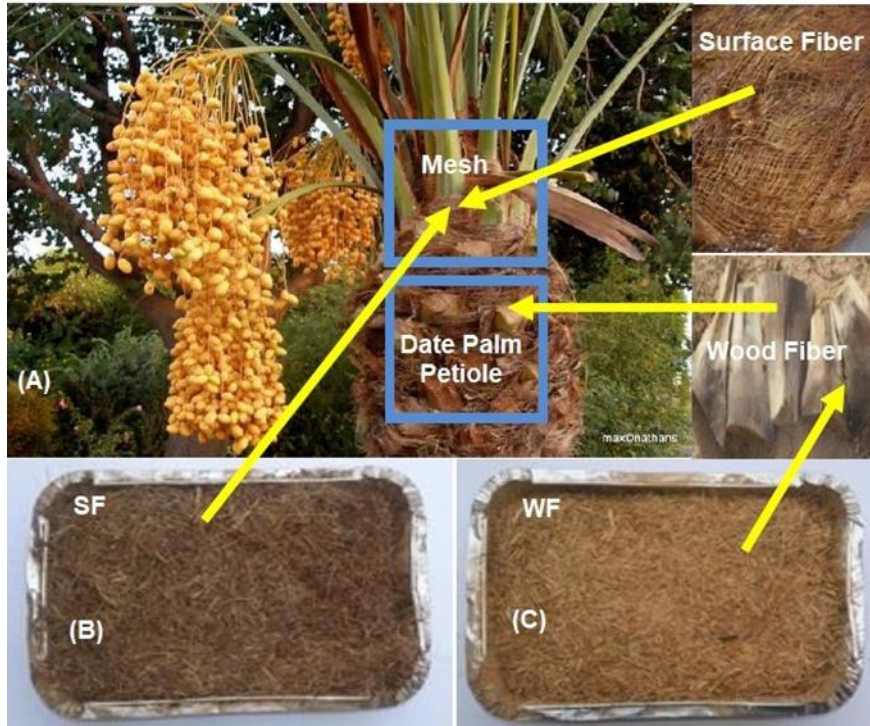
Figure 1. Photographs of a date palm tree: (A) surface fiber and wood fiber, (B) crushed surface fiber, and (C) crushed wood fiber.

2.1. Raw materials

To produce the composites to be explored, we used the same procedure presented by Belakroum et al. (2018). The used binder is the lime produced at Saida (Algeria) (Belakroum et al., 2017). For each mixture, samples are produced by mixing date palm fiber and lime, then gradually adding water until getting a homogeneous mixture. The amount of mixing water is estimated based on the following expression:

$$m_w = m_L^w + m_F^w \tag{1}$$

where m_w is the mass of mixing water, m_L^w is the mass of water needed to hydrate lime, and

m_F^w the mass of water absorbed by palm date fibers.

As observed in Figure 2, after 30 (min), the surface fiber as well as the wood fiber are almost saturated and their water absorption rates are 1 and 1.6, respectively. Therefore, the absorbed

water mass is for surface fiber $m_{SF}^{W} = 1\,m_{F}$, and for wood fiber $m_{WF}^{W} = 1.6\,m_{F}$, where m_{F} is the fiber mass.
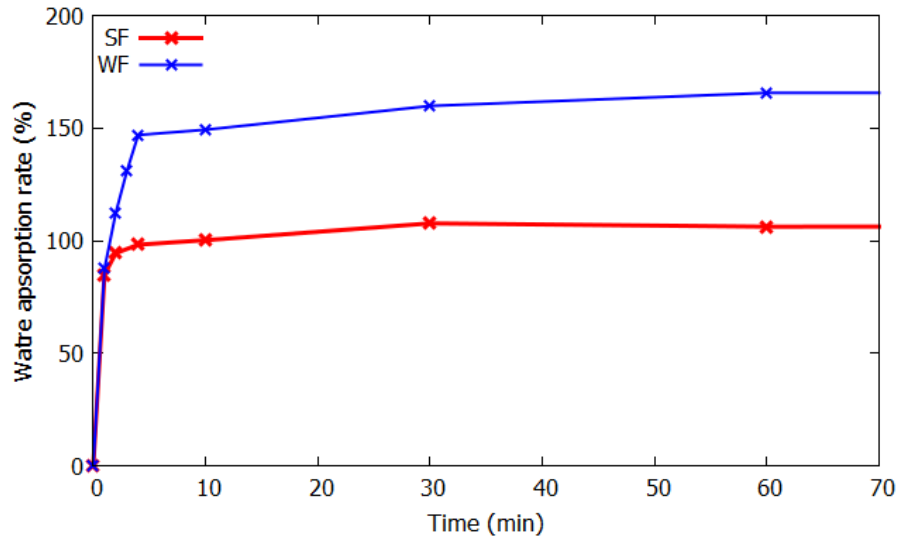
**Figure 2.** Water absorption rate vs. immersion time of date palm fibers.

Granulometric analysis allows for determining and observing the various grain diameters that constitute an aggregate. To do this, the analysis involves separating and classifying these grains according to their diameter using sieves. Isolated grains can be weighed to determine the proportion of each in the aggregate. The graphical representation of the analysis, is invaluable for observing and exploiting this information. Granulometric curves of the crushed SF and WF are shown in Figure 3. The granulometric analysis was conducted according to the French standard NF P18-304.

2.2. Bio-based composites

The studied lightweight composites are designed for the building insulation sector. Construction elements made from these materials must be easy to handle and have acceptable mechanical properties. Increasing the amount of fiber in this type of composites has a negative effect on the mechanical strength. It was noted by Belakroum et al. (2018) that the

mechanical properties for samples of 50 % DPF remain sufficient to ensure safe handling. For each type of fiber (SF or WF), three mixtures are prepared with 20, 35 and 50 % of DPF in mass. The produced samples are labeled based on the nature and the percentage of fiber:

- Surface fiber and lime is labeled SFL-%.

- Wood fiber and lime is labeled WFL-%.
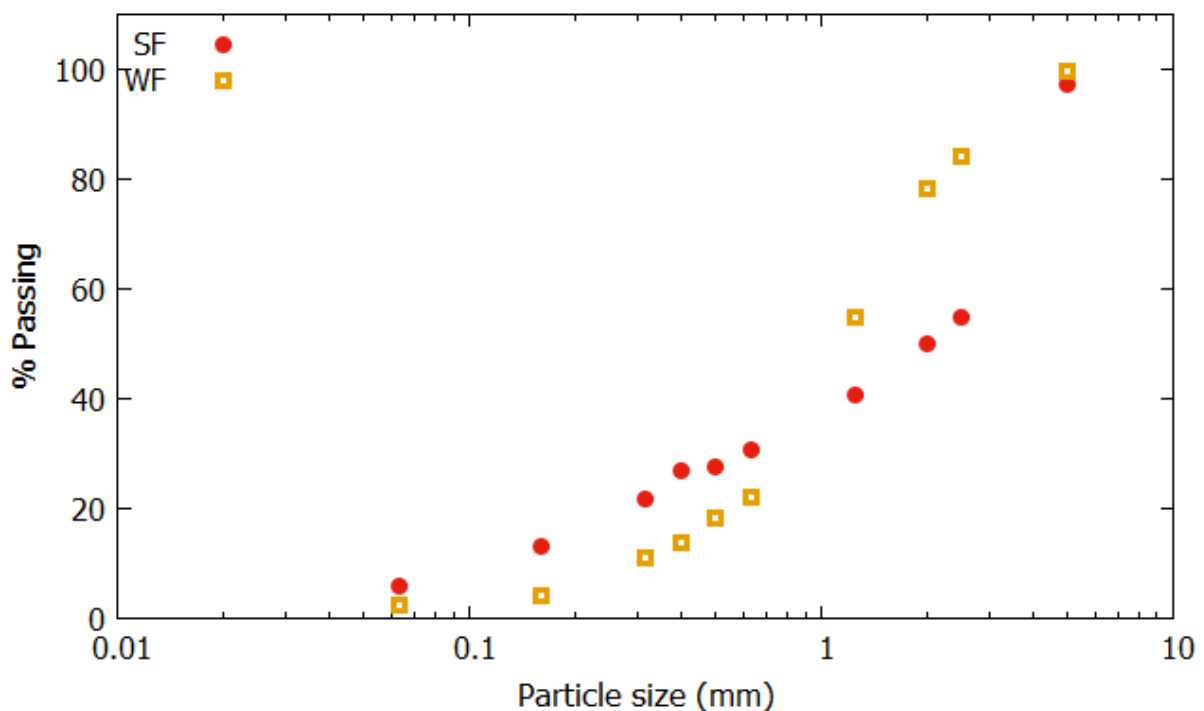
Figure 3. Granulometric curves of crushed SF and WF.

2.3. Measurement methods

2.3.1. Density and porosity measurement

Cylindrical specimens of 100mm diameter and 30mm thickness were prepared and five samples of each formulation were tested. The porosity is defined as the total volume fraction occupied by voids. The porosity is measured by a hydrostatic weighing method. The samples are first partially dried at a temperature of 60 °C and then weighed to determine their dry mass. Next, the samples are placed in a vacuum bell jar where the pressure is reduced to 12 mmHg and maintained constant for 2 hours. Subsequently, water is introduced into the bell jar

until the samples are completely submerged, and they are left for 24 hours at atmospheric pressure. At the end of this period, measurements of the saturated mass and hydrostatic mass are carried out.

The open porosity P (%) can be evaluated by the formula (Boussetoua et al., 2017; Gonen & Yazicioglu, 2007).

$$P = \frac{w_a - w_d}{w_a - w_w} \qquad (2)$$

where w_a is the specimen weight in air of saturated sample, w_w is the specimen weight in water, and w_d is the specimen dry weight after a stabilization phase in an oven regulated at 60 (°C) and 15 % RH, for 20 days.

The apparent density is calculated by:

$$\rho = \frac{w_d}{w_a - w_w} \times 1000 \qquad (3)$$

2.3.2. Thermal characterization

For the measurement of thermal properties, the dynamic measurement method was applied. The measuring device used in this study is an ISOMET 2114 portable device using a needle probe. This device applies a dynamic measurement method based on the analysis of the temperature response of the tested material to heat flow pulses. Measurements are performed on cubic samples of dimensions $100 \times 100 \times 100 \, mm^3$. All the measurements were carried out for 6 samples for each composition. The measurement accuracy is 5 % for thermal conductivity and 15 % for volume heat capacity (Belakroum et al., 2018).

During the measurement procedure, after undergoing a partial drying phase in an oven set at 60 °C, the samples are meticulously sealed within plastic bags. This step serves two critical purposes: firstly, it effectively prevents any moisture exchange with the surrounding environment. Secondly, it ensures the uniform distribution of humidity throughout the

samples, which is essential for precise measurements. It's worth noting that the mean temperature of the samples stabilizes at approximately 27 °C during this process.

Date palm fiber thermal properties characterization plays a crucial role in optimizing composite materials for specific applications, as it directly affects their performance and efficiency. The thermal conductivity of bulk fibers, especially in materials with large porosity, is crucial for understanding the overall thermal properties of composite materials containing these fibers. Fibers act as pathways for heat conduction within composite materials. The thermal conductivity of these fibers determines how efficiently heat can be transferred through them. High thermal conductivity fibers facilitate faster heat transfer, whereas low conductivity fibers impede it. To evaluate the thermal properties of pure crushed date palm fiber, the dried fiber is meticulously arranged within a glass bowl and covered with plastic wrap.

2.3.3. Vapor permeability

The water vapor permeability characterizes the ability of a material to transfer moisture under a vapor pressure gradient once the steady state is reached (Mazhoud et al., 2016). Vapor permeability is measured according to the European standard NF EN ISO 12572. The principle of this method is to impose to samples of a constant thickness a one-dimensional vapor pressure gradient in a controlled isothermal environment (at 23°C). In this study, four cylindrical specimens with a diameter of 100mm and a thickness of 32mm were explored for each composition. A stabilization phase of the specimens must be performed before starting the measurements. This is carried out by introducing the samples into a climatic chamber set at 23 (°C) and 50 % RH until the mass becomes stable, with a variation of three successive weighings not exceeding 5 %. Each sample is insulated on its lateral sides with a waterproof adhesive and fixed on a cup containing a saline solution . The cups and samples are then placed in a climatic chamber set at suitable temperature and humidity. Four samples for each

formulation are tested for both dry and wet cups. For the dry cup, the 0 % RH environment is created by an anhydrous calcium dichloride $CaCl_2$. For the wet cup, an atmosphere of 94 % RH is ensured by a saturated salt solution of potassium nitrate KNO_3. To create the humidity gradient, the cups are placed in a climatic chamber set at 23 (°C) and 50 % RH. The devices are weighed periodically to determine the weight gain (or loss) of the cups Δm. The mass variation rate G is calculated by:

$$G = \frac{\Delta m}{\Delta t} \tag{4}$$

The water vapor permeability π (kg.m^{-1}.s^{-1}.Pa^{-1}) and the material vapor resistance factor μ were estimated as follows:

$$\pi = \frac{G \times e}{\Delta p_v \times A} = W \times e \tag{5}$$

$$\mu = \frac{\pi_a}{\pi} \tag{6}$$

Where $\pi_a = 2 \times 10^{-10}$ kg.m^{-1}.s^{-1}Pa^{-1} is the air vapor permeability, Δp_v (Pa) is the vapor pressure gradient, A (m^2) is the exposed surface area, W (kg.m^{-2}.s^{-1}.Pa^{-1}) is the permeance, and e (m) is the specimen thickness.

For temperatures above 0°C, the vapor pressure on each side of a test specimen can be calculated using the temperature T (°K) and relative humidity φ (%RH), as described by the following formula:

$$p_v = \varphi \times 610.5 \times e^{\frac{17.269 \times T}{273.3 + T}} \tag{7}$$

The air layer between the specimen and the saline solution presents resistance to the flow of water vapor for most materials. While this resistance is generally lower than that of the material itself, it may lead to a significant error, particularly in the case of highly permeable

materials or thin membranes. Following are the corrections needed to the permeance W if the equivalent air thickness for water vapor diffusion $S_d = \mu \times e$ is less than 0.2 m:

$$W_c = \frac{1}{\dfrac{A \ \Delta p_v}{G} - \dfrac{d_a}{\pi_a}}$$ (8)

d_a (m) is the thickness of the air layer.

To minimize the influence of the air layer above the test cup when testing highly permeable materials, it is crucial to ensure that the test cups are positioned to maintain an air velocity of at least 2 m/s above each cup.

2.3.4. Sorption curve

The European standard EN NF ISO 12571 specifies the procedures for experimentally determining the adsorption-desorption curves of thermal insulating materials by using the climatic chamber method. Initially, three samples measuring 100 mm x 100 mm with a thickness of 30 mm are partially dried in a ventilated oven at 60 °C and maintained at less than 10% relative humidity (RH). The criterion for achieving constant mass is met when the change in mass of the test specimens over a 24-hour period is less than 0.1% of the total mass. To find the adsorption scanning isotherm, the samples are put in a climate chamber that is kept at a constant temperature of 23 ± 0.1 °C and successively exposed to relative humidity levels of 20 ± 2 %, 33 ± 2 %, 43 ± 2%, 75 ± 2%, 90 ± 2%, and 94 ± 2%. Mass evolution is measured with an accuracy of 0.001 g. The weighing of the samples is performed manually every 24 hours. Equilibrium is considered achieved when the mass variation does not exceed 0.1% within 24 hours for three consecutive days.

The water content w is calculated according to:

$$w = \frac{m - m_0}{m_0} = \frac{m_w}{m_0}$$ (9)

where m is the wet specimen mass (g), m_0 is the dry specimen mass, and m_w is the water content mass (g).

Several models have been developed in the literature to describe the relationship between the relative humidity of air and the moisture content in porous materials (Aït Oumeziane et al., 2016; Collet et al., 2013; Latif et al., 2014). In this study, we used the EMPD model for fitting sorption curves (Woods & Winkler, 2018). The equilibrium moisture sorption curve can be defined by the following general equation:

$$w = a \varphi^b + c \varphi^d \tag{10}$$

where $a, b, c,$ and d are fitting parameters and φ is the relative humidity.

3. Results and discussion

3.1. Density and porosity

The measured density and porosity are summarized in Table 1. It is observed that specimens based on wood fiber are more porous than those based on surface fiber. For the two types of composites (SFL and WFL) the apparent density decreases with increasing DPF percentage. For the same fiber content, inserting surface fiber in lime produces specimens of greater density than wood fiber.

Table 1. Open porosity and apparent density of different composition.

Sample	Open porosity %	Standard deviation	Apparent density (kg/m^3)	Standard deviation
SFL-20%	51	1.1	1199	25.6
SFL-35%	52	0.3	801	8.4
SFL-50%	55	0.6	619	19.2
WFL-20%	57	0.2	841	19.6
WFL-35%	58	0.6	775	18.7
WFL-50%	64	0.5	608	9.2

3.2. Thermal properties

At first, thermal conductivity, specific heat capacity, and thermal diffusivity of pure dry date palm fibers were measured. According to the Table 2, the thermal conductivities of the two types of fiber are almost the same and having a value of about 0.06 (W/(m·K)). However, it can be observed that the specific heat capacity, and therefore the thermal diffusivity, differ according to the type of fiber. We note that the surface fiber presents a higher thermal capacity than the wood fiber. The highest thermal diffusivity recorded is that for wood fiber. Therefore, in unsteady state wood fiber is thermally more diffusive than surface fiber. The recorded conductivities are significantly lower than those published by Agoudjil et al. (2011). Their results showed an average thermal conductivity of 0.083 (W/(m·K)) for date palm woods. This difference is due to the dense nature of the date palm wood compared to crushed fiber and therefore to the difference of densities. On the other hand, the obtained thermal diffusivities for SF and WF are higher than palm wood thermal diffusivity ranging from $2.2x10^{-7}$ (m^2/s) to $3.2x10^{-7}$ (m^2/s).

An interesting review of some unconventional sustainable building insulation materials is presented in reference (Asdrubali et al., 2015) . We can notice that SF and WF thermal conductivities are lower than those of corn cob (0.101 (W/(m·K))), pecan shells (0.0884 (W/(m·K))) and straw ball (0.067 (W/(m·K))). The results showed that date palm fiber is adequate for insulation purposes.

Table 2. Thermal properties of dried date palm fibers (SF and WF).

| Type of fiber	Conductivity (W/(m·K))	Standard deviation	Thermal capacity (J /m^3·K)	Standard deviation	Thermal diffusivity (m^2/s)	Standard deviation
SF	0.0629	$9.8x10^{-5}$	$1.78x10^5$	$5.8x10^2$	$3.54x10^{-7}$	$5.00x10^{-10}$
WF	0.0657	$1.4x10^{-4}$	$1.59x10^5$	$5x10^2$	$4.15x10^{-7}$	$9,6x10^{-10}$

For lime-based composites, Figure 4 shows the variation of thermal conductivity with respect to fiber percentage. When the date palm fiber percentage increased, we noted a significant

decrease of thermal conductivity of the explored samples. Similar behavior was reported for bio-based composites in references (Belakroum et al., 2018; Benmansour et al., 2014; Chikhi et al., 2013). It is also observed that WF-lime samples have lower thermal conductivities than SF-lime samples. For the same fiber percentage, the difference between the measured conductivities of the samples of the two types of used fibers (SF and WF) decreases with the increase of fiber content. For 20 % fiber the difference is 36.68 % while at 50 % fiber the difference becomes 15.47 %. The two lowest thermal conductivities found are 0.108 (W/(m.K)) for WFL-50 % and 0.128 (W/(m.K)) for SFL-50 %.
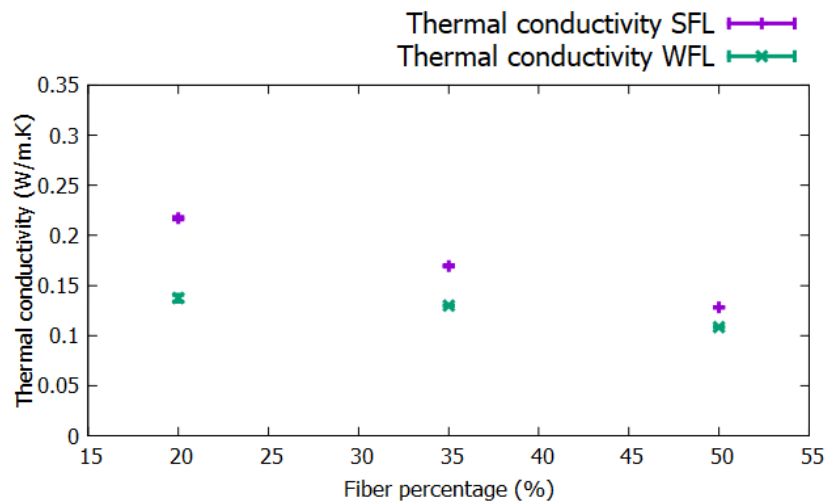
Figure 4. Variation of thermal conductivity with respect to fiber percentage.

Figure 5 depicts the evolution of the thermal diffusivity as a function of date palm fiber percentage. It can be noticed that the incorporation of date palm fiber leads to a decrease in composites thermal diffusivity. Thus, the more the composite contains date palm fiber, the less it allows heat diffusion. This behavior is very important in thermal insulation, as a good insulation material should not only have a low thermal conductivity but must also allow delaying heat transmission (Boumhaout et al., 2017). As observed, for fiber percentages of 20 % and 35 % samples based on surface fiber allow better heat diffusion than those based on wood fiber. On the other hand, we note that at 50 % fiber the two types of composites have indeed equal thermal diffusivities of 0.26 (m/s^2).
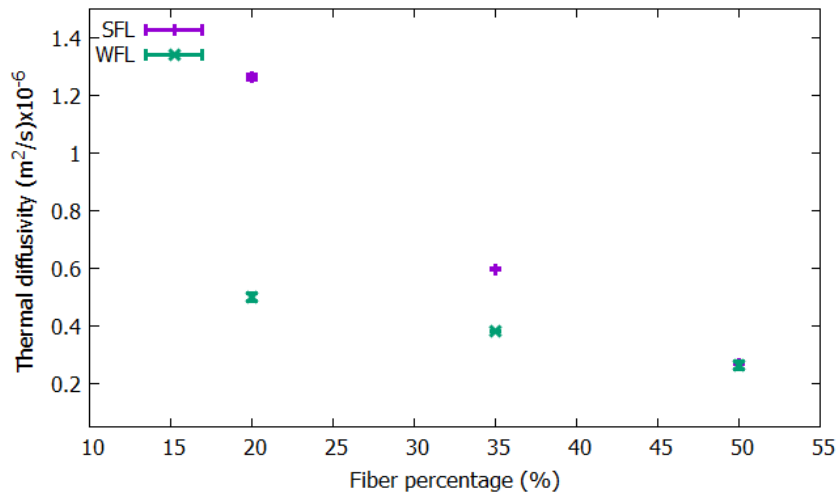
Figure 5. Variation of thermal diffusivity with respect to fiber percentage.

3.3. Vapor permeability

The water vapor permeability and resistance factor of the elaborated DPF-lime composites are summarized in table 3. It is clear that vapor permeability increases with the increase of fiber percentage. The largest vapor permeability values are recorded for the samples based on wood fiber and lime. This can be justified by the larger open porosities recorded for these specimens (table 1). It is important to underline that the macro-pores located between natural fibers have a significant influence on water vapor permeability, compared to the micro-pores which are present within the binder (Haba et al., 2017). It is also observed that vapor permeability of dry cup is always lower than that obtained on wet cup. This is expected since vapor permeability is moisture dependent and the value of vapor permeability rises with the increase of moisture content of insulation materials (Latif et al., 2014).

Table 3. Water vapor permeability π and water vapor resistance factor μ of the studied composites.

| Sample	Dry cup		Wet cup	
	Permeability$\pi \times 10^{-11}$ (kg /m·s·Pa)	μ	Permeability$\pi \times 10^{-11}$ (kg /m·s·Pa)	μ
SFL-20%	2.14	9.11	3.65	5.35
SFL-35%	2.24	8.71	4.18	4.66
SFL-50%	2.59	7.52	4.46	4.38
WFL-20%	2.35	8.30	3.56	5.48
WFL-35%	3.15	6.19	3.63	5.37
WFL-50%	3.72	5.25	4.08	4.78

3.4. Adsorption scanning isotherms

Adsorption scanning isotherms of all studied date palm fiber and lime composites are presented in Figure 6. The curves' shape is comparable to other composites made of natural fibers described in the literature like hemp-lime (Mazhoud et al., 2016) and wheat straw (Ismail et al., 2022) biocomposites. The results obtained at each relative humidity values are completed by error bars and fitted using the EMPD model. The adsorption fitted curve shows good agreement with the experimental data for the humidity range of 20 %–94 % RH. The evolution of the water content in adsorption is not similar for the different explored mixtures. It is clear that the ability for absorbing moisture improves with increasing fiber content. The specimens that have demonstrated the best performance are SFL-50 % and WFL-50 %. All EMDP model-fitting parameters for all the studied mixtures are summarized in Table 4.

It is crucial to acknowledge that residual moisture present in biocomposites, resulting from incomplete drying, significantly affects their adsorption isotherms. This phenomenon was observed by Colinart et al. (2020) in their investigation of the hygrothermal properties of light-earth building materials. The existence of residual moisture within a sample causes an overestimation of its dry mass. Consequently, this leads to an underestimation of the actual
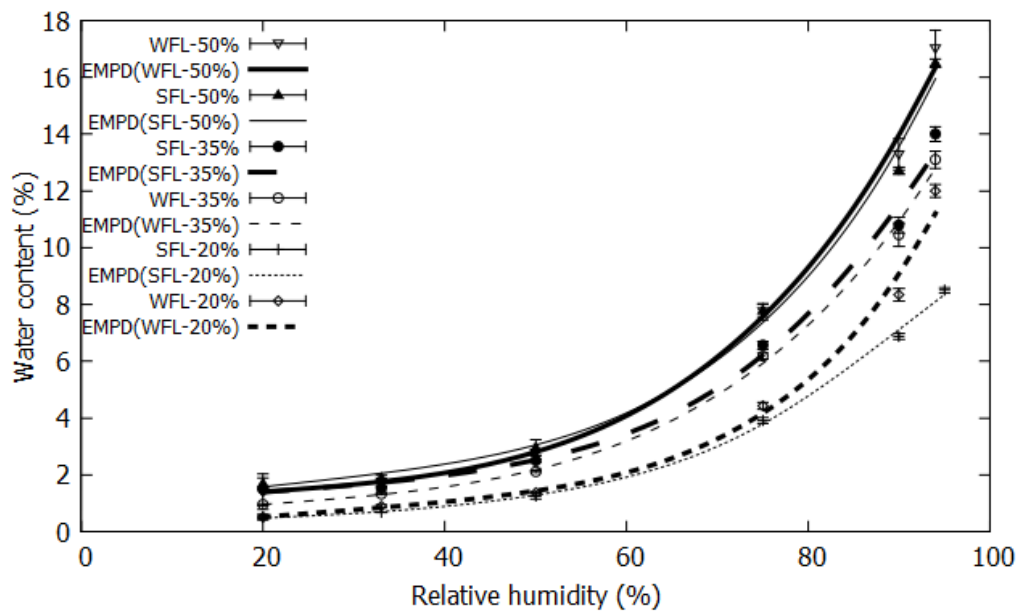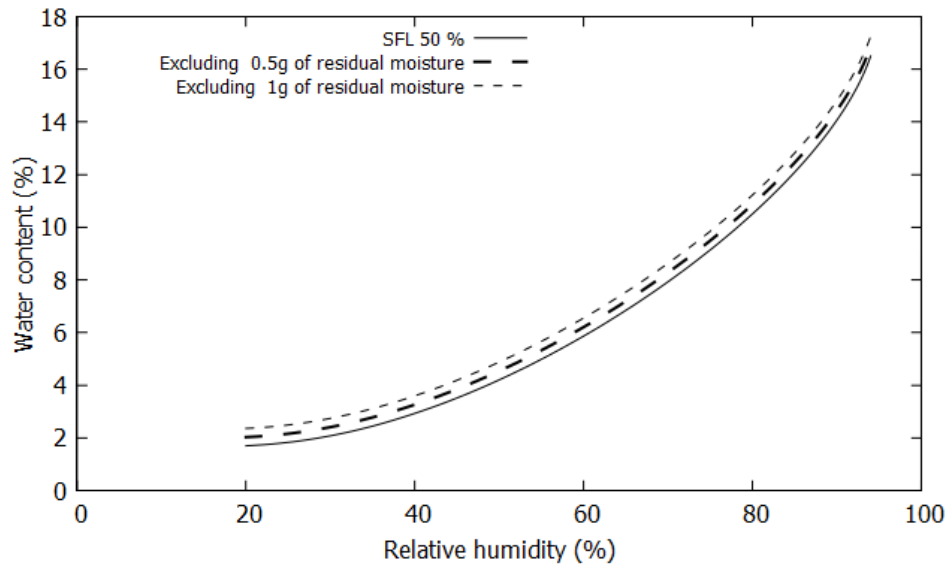
Figure 6. Adsorption scanning curves of the studied SF-lime and WF-lime samples: comparison of experimental measurements with adsorption curves fitted by the EMPD model.

Table 4. Fitting parameters of the EMDP model (adsorption scanning curves for the studied specimens).

Composites	Specimens	a	b	c	d
Surface fiber and lime	SFL-20%	0.094	4.149	0.011	0.525
	SFL-35%	0.154	4.074	0.015	0.544
	SFL-50%	0.032	0.437	0.171	4.579
Wood fiber and lime	WFL-20%	0.023	0.930	0.130	5.863
	WFL-35%	0.019	0.433	0.142	4.181
	WFL-50%	0.184	4.121	0.021	0.259

Figure 7. Adsorption scanning curves of the specimen SFL-50% for different considered residual moisture weights.

Finally based on the results of the experiments conducted in this study, it has been observed that composites made from date palm fibers and lime exhibit thermal and hygroscopic properties that vary depending on their fiber content. The most significant hygrothermal properties have been measured, paving the way for the development of mathematical models for evaluating coupled heat and mass transfers through these biomaterials.

4. Conclusion

In this study, the hygrothermal properties of biobased composites based on date palm fiber and lime were explored experimentally. Two types of DPF were used: SF and WF. Their measured heat transport properties showed their suitability for thermal insulation purposes. For the studied mixtures, it is observed that WF-lime samples have lower thermal conductivities than SF-lime samples. The two lowest thermal conductivities found are 0.108 W/m·K for WFL-50%, and 0.128 W/m·K for SFL-50 %. It is found that the more composites contain SF or WF, the lower the thermal diffusivity. The specimens WFL-50 %, and SFL-50 % have indeed equal thermal diffusivities of 0.26 m/s^2. This proves that these materials can

still be considered as insulation materials. All samples exhibited high water vapor permeability, and the highest values were observed for samples with 50% fiber. Utilizing a rigorous experimental approach, we systematically analyze the moisture sorption characteristics for different fiber percentage. Notably, for all studied compositions, we establish a model based on the Effective Moisture Penetration Depth (EMPD) method, providing a comprehensive framework for understanding and predicting the moisture sorption behavior of date palm fiber and lime composites. Moreover, these measured properties can provide valuable input for numerical simulations, enabling a deeper understanding of hygrothermal dynamics in building envelopes.

Declaration of interests

The authors declare that they have no known competing financial interests or personal relationships that could have appeared to influence the work reported in this paper.

References

Agoudjil, B., Benchabane, A., Boudenne, A., Ibos, L., Fois, M. 2011. Renewable materials to reduce building heat loss: Characterization of date palm wood. *Energy and Buildings*, **43**(2–3), 491-497.

Aït Oumeziane, Y., Moissette, S., Bart, M., Lanos, C. 2016. Influence of temperature on sorption process in hemp concrete. *Construction and Building Materials*, **106**, 600-607.

Al-Oqla, F.M., Sapuan, S.M. 2014. Natural fiber reinforced polymer composites in industrial applications: feasibility of date palm fibers for sustainable automotive industry. *Journal of Cleaner Production*, **66**, 347-354.

Alotaibi, M.D., Alshammari, B.A., Saba, N., Alothman, O.Y., Sanjay, M.R., Almutairi, Z., Jawaid, M. 2019. Characterization of natural fiber obtained from different parts of date palm tree (Phoenix dactylifera L.). *International Journal of Biological Macromolecules*, **135**, 69-76.

Asdrubali, F., D'Alessandro, F., Schiavoni, S. 2015. A review of unconventional sustainable building insulation materials. *Sustainable Materials and Technologies*, **4**, 1-17.

Asim, M., Jawaid, M., Fouad, H., Alothman, O.Y. 2021. Effect of surface modified date palm fibre loading on mechanical, thermal properties of date palm reinforced phenolic composites. *Composite Structures*, **267**, 113913.

Asim, M., Jawaid, M., Khan, A., Asiri, A.M., Malik, M.A. 2020. Effects of Date Palm fibres loading on mechanical, and thermal properties of Date Palm reinforced

phenolic composites. *Journal of Materials Research and Technology*, **9**(3), 3614-3621.

Asyraf, M.R.M., Ishak, M.R., Syamsir, A., Nurazzi, N.M., Sabaruddin, F.A., Shazleen, S.S., Norrrahim, M.N.F., Rafidah, M., Ilyas, R.A., Rashid, M.Z.A., Razman, M.R. 2022. Mechanical properties of oil palm fibre-reinforced polymer composites: a review. *Journal of Materials Research and Technology*, **17**, 33-65.

Atiki, E., Taallah, B., Feia, S., Almeasar, K.S., Guettala, A. 2021. Effects of Incorporating Date Palm Waste as a Thermal Insulating Material on the Physical Properties and Mechanical Behavior of Compressed Earth Block. *Journal of Natural Fibers*, 1-18.

Belakroum, R., Gherfi, A., Bouchema, K., Gharbi, A., Kerboua, Y., Kadja, M., Maalouf, C., Mai, T.H., El Wakil, N., Lachi, M. 2017. Hygric buffer and acoustic absorption of new building insulation materials based on date palm fibers. *Journal of Building Engineering*, **12**, 132-139.

Belakroum, R., Gherfi, A., Kadja, M., Maalouf, C., Lachi, M., El Wakil, N., Mai, T.H. 2018. Design and properties of a new sustainable construction material based on date palm fibers and lime. *Construction and Building Materials*, **184**, 330-343.

Bellatrache, Y., Ziyani, L., Dony, A., Taki, M., Haddadi, S. 2020. Effects of the addition of date palm fibers on the physical, rheological and thermal properties of bitumen. *Construction and Building Materials*, **239**, 117808.

Benaimeche, O., Carpinteri, A., Mellas, M., Ronchei, C., Scorza, D., Vantadori, S. 2018. The influence of date palm mesh fibre reinforcement on flexural and fracture behaviour of a cement-based mortar. *Composites Part B: Engineering*, **152**, 292-299.

Benmansour, N., Agoudjil, B., Gherabli, A., Kareche, A., Boudenne, A. 2014. Thermal and mechanical performance of natural mortar reinforced with date palm fibers for use as insulating materials in building. *Energy and Buildings*, **81**, 98-104.

Boukhattem, L., Boumhaout, M., Hamdi, H., Benhamou, B., Ait Nouh, F. 2017. Moisture content influence on the thermal conductivity of insulating building materials made from date palm fibers mesh. *Construction and Building Materials*, **148**, 811-823.

Boumhaout, M., Boukhattem, L., Hamdi, H., Benhamou, B., Ait Nouh, F. 2017. Thermomechanical characterization of a bio-composite building material: Mortar reinforced with date palm fibers mesh. *Construction and Building Materials*, **135**(Supplement C), 241-250.

Boussetoua, H., Maalouf, C., Lachi, M., Belhamri, A., Moussa, T. 2017. Mechanical and hygrothermal characterisation of cork concrete composite: experimental and modelling study. *European Journal of Environmental and Civil Engineering*, 1-16.

Braiek, A., Karkri, M., Adili, A., Ibos, L., Ben Nasrallah, S. 2017. Estimation of the thermophysical properties of date palm fibers/gypsum composite for use as insulating materials in building. *Energy and Buildings*, **140**, 268-279.

Chennouf, N., Agoudjil, B., Boudenne, A., Benzarti, K., Bouras, F. 2018. Hygrothermal characterization of a new bio-based construction material: Concrete reinforced with date palm fibers. *Construction and Building Materials*, **192**, 348-356.

Chikhi, M., Agoudjil, B., Boudenne, A., Gherabli, A. 2013. Experimental investigation of new biocomposite with low cost for thermal insulation. *Energy and Buildings*, **66**, 267-273.

Colinart, T., Vinceslas, T., Lenormand, H., Menibus, A.H.D., Hamard, E., Lecompte, T. 2020. Hygrothermal properties of light-earth building materials. *Journal of Building Engineering*, **29**, 101134.

Collet, F., Chamoin, J., Pretot, S., Lanos, C. 2013. Comparison of the hygric behaviour of three hemp concretes. *Energy and Buildings*, **62**, 294-303.

Gonen, T., Yazicioglu, S. 2007. The influence of compaction pores on sorptivity and carbonation of concrete. *Construction and Building Materials*, **21**(5), 1040-1045.

Haba, B., Agoudjil, B., Boudenne, A., Benzarti, K. 2017. Hygric properties and thermal conductivity of a new insulation material for building based on date palm concrete. *Construction and Building Materials*, **154**, 963-971.

Ismail, B., Belayachi, N., Hoxha, D. 2022. Hygric properties of wheat straw biocomposite containing natural additives intended for thermal insulation of buildings. *Construction and Building Materials*, **317**, 126049.

Kannan, G., Thangaraju, R. 2021. Recent Progress on Natural Lignocellulosic Fiber Reinforced Polymer Composites: A Review. *Journal of Natural Fibers*, 1-32.

Latif, E., Tucker, S., Ciupala, M.A., Wijeyesekera, D.C., Newport, D. 2014. Hygric properties of hemp bio-insulations with differing compositions. *Construction and Building Materials*, **66**, 702-711.

Mahdi, E., Ochoa, D., Vaziri, A., Eltai, E. 2019. Energy absorption capability of date palm leaf fiber reinforced epoxy composites rectangular tubes. *Composite Structures*, **224**, 111004.

Mazhoud, B., Collet, F., Pretot, S., Chamoin, J. 2016. Hygric and thermal properties of hemp-lime plasters. *Building and Environment*, **96**, 206-216.

Subramanian, G.K.M., Balasubramanian, M., Jeya Kumar, A.A. 2021. A Review on the Mechanical Properties of Natural Fiber Reinforced Compressed Earth Blocks. *Journal of Natural Fibers*, 1-15.

Supian, A.B.M., Jawaid, M., Rashid, B., Fouad, H., Saba, N., Dhakal, H.N., Khiari, R. 2021. Mechanical and physical performance of date palm/bamboo fibre reinforced epoxy hybrid composites. *Journal of Materials Research and Technology*, **15**, 1330-1341.

Taallah, B., Guettala, A. 2016. The mechanical and physical properties of compressed earth block stabilized with lime and filled with untreated and alkali-treated date palm fibers. *Construction and Building Materials*, **104**, 52-62.

Taallah, B., Guettala, A., Guettala, S., Kriker, A. 2014. Mechanical properties and hygroscopicity behavior of compressed earth block filled by date palm fibers. *Construction and Building Materials*, **59**, 161-168.

Vantadori, S., Carpinteri, A., Zanichelli, A. 2019. Lightweight construction materials: Mortar reinforced with date-palm mesh fibres. *Theoretical and Applied Fracture Mechanics*, **100**, 39-45.

Woods, J., Winkler, J. 2018. Effective moisture penetration depth model for residential buildings: Sensitivity analysis and guidance on model inputs. *Energy and Buildings*, **165**, 216-232.

Zanichelli, A., Carpinteri, A., Fortese, G., Ronchei, C., Scorza, D., Vantadori, S. 2018. Contribution of date-palm fibres reinforcement to mortar fracture toughness. *Procedia Structural Integrity*, **13**, 542-547.